Earth and Planetary Science Letters 471 (2017) 19–31

Contents lists available at ScienceDirect

Earth and Planetary Science Letters

www.elsevier.com/locate/epsl

Debris-covered glacier anomaly? Morphological factors controlling changes in the mass balance, surface area, terminus position, and snow line altitude of Himalayan glaciers

Franco Salerno [a,*], Sudeep Thakuri [b], Gianni Tartari [a], Takayuki Nuimura [c], Sojiro Sunako [d], Akiko Sakai [d], Koji Fujita [d]

[a] National Research Council, Water Research Institute (IRSA-CNR), Brugherio, Italy
[b] Central Department of Environmental Science, Tribhuvan University, Kirtipur, Nepal
[c] Faculty of Risk and Crisis Management, Chiba Institute of Science, Choshi 288-0025, Japan
[d] Graduate School of Environmental Studies, Nagoya University, Nagoya 464-8601, Japan

ARTICLE INFO

Article history:
Received 15 December 2016
Received in revised form 18 April 2017
Accepted 24 April 2017
Available online xxxx
Editor: A. Yin

Keywords:
debris-cover glaciers
mass balance
SLA
supraglacial pond density
glacier surface gradient

ABSTRACT

What are the main morphological factors that control the heterogeneous responses of debris-covered glaciers to climate change in the southern central Himalaya? A debate is open whether thinning rates on debris-covered glaciers are comparable to those of debris-free ones. Previous studies have adopted a deterministic approach, which is indispensable, but is also limiting in that only a few glaciers can be monitored. In this context, we propose a statistical analysis based on a wider glacier population as a complement to these deterministic studies. We analysed 28 glaciers situated on the southern slopes of Mt. Everest in the central southern Himalaya during the period 1992–2008. This study combined data compiled by three distinct studies for a common period and population of glaciers for use in a robust statistical analysis. Generally, surface gradient was the main morphological factor controlling the features and responses of the glaciers to climate change. In particular, the key points that emerged are as follows. 1) Reduced downstream surface gradient is responsible for increased glacier thinning. 2) The development of supraglacial ponds is a further controlling factor of glacier thinning: where supraglacial ponds develop, the glaciers register further surface lowering. 3) Debris coverage and thickness index were not found to be significantly responsible for the development of supraglacial ponds, changes in elevation, or shifts in snow line altitude.

Abbreviations

SLA: snow line altitude
Surf: glacier surface area
Δelev: elevation change
Δsurf: surface area change
Δterm: terminus change
ΔSLA: snow line altitude elevation shift
Debr_cover: debris coverage
Therm_resist: mean thermal resistance, as a proxy of debris thickness
Pond_dens: supraglacial pond density
Down_gradient: mean surface gradient of glacier downstream
Up_gradient: mean surface gradient of glacier upstream
Mean _gradient: mean surface gradient of the overall glacier
Min_elev, Mean_elev, Max_elev: minimum, mean and maximum glacier elevations
Mean_dev_from_south: the mean glacier orientation is investigated here as mean deviation from south

1. Introduction

Glaciers in the Hindu Kush and Himalaya are thinning and receding. Changes in glacier volume are driven by climate variations, particularly changes in atmospheric temperature and precipitation amount and phase, and are modified by ice flow (Bolch et al., 2012; Kääb et al., 2012). Among regions, differences in recent glacier evolution can often be associated with the respective climatic regimes (e.g., Fujita and Nuimura, 2011), particularly the varying influence of the south Asian monsoon and westerly disturbances (e.g., Yao et al., 2012). Even within the same climatic region, however, the rate of glacier changes can also be heteroge-

* Corresponding author.
E-mail address: salerno@irsa.cnr.it (F. Salerno).

http://dx.doi.org/10.1016/j.epsl.2017.04.039

neous. Many recent studies have highlighted the spatially heterogeneous distribution of glacier wastage in the Himalayas (Scherler et al., 2011a; Fujita and Nuimura, 2011; Bolch et al., 2012; Kääb et al., 2012).

A primary focus of current research is on the effect of supraglacial debris cover on glacier response to climate. Scherler et al. (2011a) estimate that 93% of glaciers in the Himalayas have debris-covered areas >20%. Between 1962 and 2011, the debris coverage of glaciers increased by $17.6 \pm 3.1\%$ in the Mt. Everest region (Thakuri et al., 2014), and this value could increase further in the future (Rowan et al., 2015). Many authors consider that a debris layer insulates the glacier surface from the atmosphere when it reaches a sufficient thickness and complicates the response to climate change compared to clean-ice glaciers (e.g., Kirkbride and Deline, 2013; Vincent et al., 2016). Consequently, the ice melt rates are reduced as less surface heat is conducted through the debris layer and transferred to the ice (e.g., Fujita and Sakai, 2014; Ragettli et al., 2015; Soncini et al., 2016). However, the effect of debris on the surface mass balance of glaciers remains unclear. Recent large-scale geodetic studies based on remotely sensed data have provided evidence that the present-day surface lowering rates of some debris-covered glacier areas in the Hindu-Kush–Himalaya may be similar to those of debris-free areas even within the same altitudinal range (e.g., Kääb et al., 2012; Nuimura et al., 2012; Ragettli et al., 2016).

In general, the thinning of debris-covered glaciers at rates similar to those of clean glaciers is referred as the "debris-covered glacier anomaly" (Pellicciotti et al., 2015; Vincent et al., 2016). Some studies hypothesized that this similarity could be due to mechanisms such as the formation of supra-glacial ponds, ice cliffs, and englacial hydrological processes that may act as a catalyst for melt (e.g., Sakai et al., 2000, 2002; Buri et al., 2015; Miles et al., 2016), while other authors consider that the insulating effect of debris cover has a larger effect on total mass loss than the enhanced ice ablation due to supraglacial ponds and exposed ice cliffs (e.g., Hambrey et al., 2008; Vincent et al., 2016).

In this context, this study aims to contribute to this debate by carrying out a statistical analysis of 28 glaciers with varying debris coverage (from 0 to 66%, total area 360 km^2 in 1992) situated on the southern slopes of Mt. Everest (central southern Himalaya) during the period 1992–2008. Given that the climatic forcing should be constant over this limited area, we attempt to explain differences observed in glacier changes over the past few decades in terms of morphological predictors. In this analysis we considered four main indicators of glacier change under the recent global warming (elevation, surface area, terminus and snow line altitude, or SLA), as explanatory variables. The candidate predictors are the slope, surface gradient, aspect, and elevation of glaciers. Considering the relevance of the topic, the spatial debris coverage, proxy of debris thickness and density of supraglacial ponds on the downstream areas of these glaciers are also considered in the analysis.

The question we pose here is, "What are the main morphological factors controlling the observed heterogeneous responses of debris-covered glaciers to climate change in the southern central Himalaya?" We attempt to answer to this question by analysing a dataset derived from three recently published studies (Nuimura et al., 2012; Salerno et al., 2012; Thakuri et al., 2014). The novel contribution of this study is that it combines a variety of morphological data collected for the same glaciers over the same study period in a unique statistical analysis. These data include the main variables that should be considered to answer the research question: thinning rates (Nuimura et al., 2012), pond density (Salerno et al., 2012), and glacier and debris area changes (Thakuri et al., 2014). Moreover, we provide here to derive the thermal resistance of debris cover surfaces from remotely sensed data as a proxy of debris thickness.

2. Region of investigation

The current study is focused on the southern Koshi (KO) Basin, which is located in the eastern part of the central Himalaya. In particular, the region of investigation includes glaciers belonging to the Sagarmatha (Mt. Everest) National Park (SNP) (27° 45′ to 28° 7′ N; 85° 59′ to 86° 31′ E) on the southern slopes of Mt. Everest (Fig. 1) (e.g., Tartari et al., 2008; Amatya et al., 2010). The climate here is characterized by monsoons, which have a prevailing south-north direction. The daily temperature and precipitation time series of the last twenty years (1994–2013) have been reconstructed; this time series shows that the mean annual air temperature has increased by 0.9 °C since the early 1990s (Salerno et al., 2015). Significant increases were found in spring and winter, mainly in terms of minimum daily temperatures. Regarding precipitation, a substantial reduction in rainfall (−47%) and in the probability of snowfall (−10%) has been observed in this area over the last twenty years. According to Yao et al. (2012), there is strong evidence of a general weakening of the monsoon over the Himalayas as a whole.

Many researchers have investigated the region from a glaciological perspective. Most of the large glaciers in the SNP are debris-covered, i.e., the ablation zone is partially covered with supraglacial debris (e.g., Bolch et al., 2011; Nuimura et al., 2012; Thakuri et al., 2014). More than 75% of the glacier surfaces lie between 5000 m and 6500 m a.s.l. (Thakuri et al., 2014). The glaciers are considered as summer-accumulation glaciers, which are fed mainly by summer precipitation from the south Asian monsoon system (e.g., Soncini et al., 2016). This region is characterized by the greatest number of supraglacial ponds in the overall Hindu Kush-Himalaya range (Gardelle et al., 2011) and many studies have shown that proglacial lakes increased after the early 1960s (Gardelle et al., 2011; Thakuri et al., 2016).

3. Data and methods

The dataset used in this analysis comes from three published studies: Thakuri et al. (2014), Nuimura et al. (2012), Salerno et al. (2012). For the detailed methodological procedures used, it is necessary to refer to these works. Here, we note the main methodological aspects.

Thakuri et al. (2014) considered glaciers larger than 1 km^2 lying within the SNP, and these glaciers had a total surface area of approximately 360 km^2 in 1992. The authors tracked $\Delta Surf$ (change in surface area), ΔSLA (change in snow line altitude) and $\Delta Term$ (change in terminus position) from 1962 to 2011, considering the intermediate dates of 1975, 1992, 2000, and 2008. Morphological parameters such as the mean slope, aspect, minimum, mean and maximum elevations, and debris coverage were also calculated for each year of analysis. All data were derived from satellite imagery, with the assistance of all available historical maps. In particular, a Landsat TM scene (Landsat-92, pixel 30 m) and an ALOS AVNIR-2 scene (ALOS-08, pixel 10 m) were used for 1992 and 2008, respectively. Both data were acquired after the monsoon season during the period of October–November (details in Thakuri et al., 2014). These images are characterized by low cloud cover and correspond to time just after the end of the snow accumulation and ablation period for that year; this allows for homogeneous comparisons. The *SLA* obtained from satellite imagery represents the transient snow line of the year that varies along the year, but remains stable after the end of summer, corresponding to the end of the ablation season (e.g., Pelto, 2011). For remotely sensed digital elevation models (DEMs), the authors used the Advanced Spaceborne

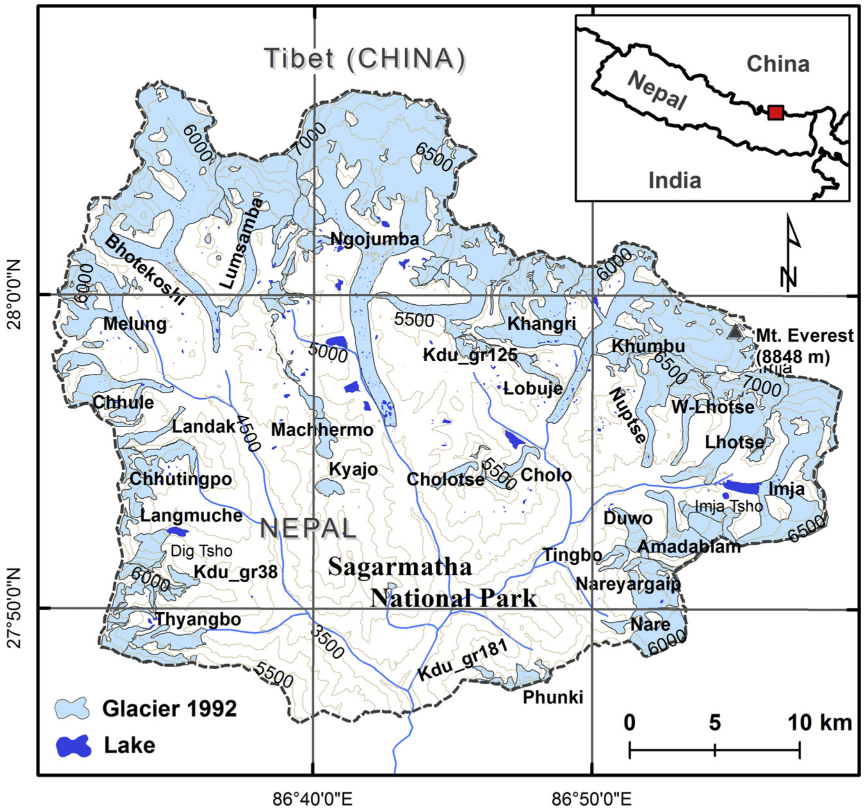

Fig. 1. Region of investigation: focused map of the Sagarmatha National Park (*SNP*) in 1992 showing the distribution of glaciers considered in this study with a surface area >1 km^2; in the up right corner the location of the *SNP*.

Thermal Emission Global Digital Elevation Model (ASTER GDEM) Version 2. The glacier outlines were manually delineated using an on-screen digitizing method based on visual interpretation and false-colour composite images developed from multispectral bands and assisted by the DEM. The band ratio (TM4/TM5) technique (Paul et al., 2004) was used to obtain a clear view of snow and ice fraction that assisted in the manual digitization. The snow lines on the glaciers were distinguished from the images as the boundary between the bright white snow and the darker ice by visual interpretation and using the FCC images. The *SLA* was then calculated for each glacier as the average altitude of the identified snow line using the DEM. The same DEM and the glacier outlines were used to derive morphological features (slope, aspect, elevation). The mean elevation, aspect, and slope of each glacier were computed as the arithmetic mean of each pixel intersected by the glacier outline. To identify and catalogue the glaciers, they followed the classification of Salerno et al. (2008). Moreover, we calculate the glacier surface gradient by calculating: 1) the angle of a line running from the lower and the highest part of the glacier surface (according to Quincey et al., 2007) (hereafter *gradient*) and 2) the mean slope of the longitudinal profile (200 m of longitudinal band), following central flow line of each glacier. Fig. S1 of Supplementary Materials presents the correlation matrix among these methods. We can note that they are significantly correlated among each other. Afterwards, we carry out all the analysis, presented in the following, applying these three methods and observing the same main findings (significant correlations). Therefore, hereafter, we decided to show only the analysis carried out with the glacier surface gradient calculated according to Quincey et al. (2007) because the observed correlations with this method were stronger.

We use the $\Delta Elev$ (change in glacier elevation) data and the relevant changes in glacier mass balance, which were estimated by Nuimura et al. (2012) from 1992 to 2008 for a region of investigation little bit larger than the SNP. The estimation was done on three DEMs calibrated with a differential GPS survey data done in 2007. The first DEM was derived from maps (Map-DEM). The Survey Department of Nepal published 1:50000 scale topographic maps from aerial photographs taken in 1992. The second DEM is a Shuttle Radar Topography Mission-derived DEM (SRTM-DEM). The third DEM is an ASTER-DEM. Terrains steeper than 30° were excluded because it leads to poor accuracy (Bolch et al., 2008; Fujita et al., 2008). The elevation changes calculated by these authors are in agreement with previous studies (Bolch et al., 2011). The elevation change was calculated only for the gentle slopes corresponding mainly to the lower parts of the glaciers. We provide here the glacier surface area of each glacier for which these authors calculated $\Delta Elev$ derived from the ASTER DEM. We considered only the $\Delta Elev$ values of those glaciers for which more than 2/3 of the total surface area was considered in the computation of the elevation change. In this way, we analysed 24 glaciers. Therefore, in Table 1 we can observe that we excluded those glaciers with the highest surface gradients, for which it is more complex to estimate elevation changes from DEMs.

Salerno et al. (2012) digitized the surface area of supraglacial ponds in 2008 on the same glaciers that were tracked successively by Thakuri et al. (2014). The supraglacial pond density (computed with respect to the downstream area of the glaciers) was calculated using an ALOS AVNIR-2 scene (ALOS-08, pixel size 10 m) referred to the post monsoon season (24 October 2008). It is well known that area and shape of each supraglacial pond shows high intra- and interannual variability (e.g., Miles et al., 2017; Gardelle et al., 2011; Watson et al., 2016). However, Miles et al. (2017) pointed out that larger ponds are highly recurrent and persistent among seasons and for multiple years. Considering that the pond population analysed in Salerno et al. (2012) represents a single scene, we found appropriate to evaluate if this dataset correctly represents the possible variability in supraglacial pond

Table 1

Dataset of morphological characteristics analyzed in this study (data comes from Nuimura et al., 2012; Salerno et al., 2012; Thakuri et al., 2014). Glacier changes are referred to the 1992–2008 period; Surface gradient data are calculated according to Quincey et al. (2007); the other morphological boundary conditions are referred to 1992. *Surf*: Glacier surface area; *SLA*: Snow line Altitude; Δ*Surf*: Surface area change; Δ*SLA*: Snow line Altitude elevation shift; Δ*Term*: terminus change; Δ*Elev*: elevation change; *Debr_cover*: Debris coverage; *Therm_resist*: thermal resistance, as a proxy of debris thickness; *Pond_dens*: Supraglacial pond density. Mean aspect, i.e., the mean glacier orientation is investigated here as mean deviation from south (*Mean_dev_from_south*).

Glacier	Glacier status		Glacier changes (explanatory variables)				Morphological boundary conditions (predictors)										
Name	*Surf* (km^2)	*SLA* (m a.s.l.)	Δ*Elev* ($m\,a^{-1}$)	Δ*Surf* (%)	Δ*Term* (m)	Δ*SLA* (m)	*Down gradient* (°)	*Up gradient* (°)	*Mean gradient* (°)	*Mean aspect* (°)	*Mean dev from south* (°)	*Mean elev* (m a.s.l.)	*Min elev* (m a.s.l.)	*Max elev* (m a.s.l.)	*Debr cover* (%)	*Therm resist* ($\times 10^{-2}$ $m^2\,K\,W^{-1}$)	*Pond dens* (%)
Amadablam	10.4	5247	0.02	−6	−142	204	7	42	16	234	54	5374	4758	6417	25	1.770	0.57
Bhotekhosi	43.2	5492	−0.76	−1	−226	408	4	13	7	174	6	5578	4739	7080	37	2.088	0.92
Chhule	9.1	5288	−0.53	−12	−321	225	7	28	13	119	61	5112	4766	6264	20	2.555	1.81
Chhutingpo	7.6	5321	–	−14	−213	48	30	28	28	140	40	5554	4905	6206	5	1.537	0.00
Cholo	1.9	5062	−0.16	−24	−89	165	26	36	30	104	76	5193	4358	6442	45	2.558	0.00
Cholotse	1.5	5183	−0.45	−1	−98	166	8	50	24	226	46	5270	4846	6301	66	1.215	0.46
Duwo	2.1	4969	−0.55	0	−99	-	10	40	25	227	47	5191	4719	6452	39	1.693	0.84
Imja	27.0	5655	−0.73	−2	–	402	4	38	20	210	30	5833	4986	8226	23	1.884	0.65
Kdu_gr125	1.5	5448	−0.13	−34	−211	−2	19	46	27	172	8	5605	5258	6097	0	1.954	0.00
Kdu_gr181	1.4	–	–	−56	–	–	27	59	43	239	59	5541	4724	6572	–	0.126	0.00
Kdu_gr38	1.6	5246	0.07	−47	−537	122	21	79	54	77	103	5478	4939	6527	2	0.915	0.00
Khangri	18.6	5432	−0.48	0	0	232	8	49	17	167	13	5605	5027	7111	30	2.322	0.82
Khumbu	38.0	5519	−0.45	1	−14	328	3	20	11	212	32	6163	4876	8260	19	1.768	1.01
Kyajo	1.2	5385	−0.56	−11	0	4	14	33	24	113	67	5385	5224	5575	–	1.621	0.00
Landak	2.0	5249	–	7	−218	28	9	71	22	130	50	5285	4737	6179	38	1.604	0.00
Langmuche	3.7	5168	0.16	−20	−231	7	25	42	36	105	75	5546	4370	6659	3	1.070	0.00
Lhotse	15.9	5425	−0.66	−3	−251	251	5	46	21	207	27	5890	4758	8467	40	2.655	0.55
Lobuche	1.7	5418	–	−1	−37	281	7	25	17	145	35	5356	4923	5997	39	3.023	2.07
Lumsamba	22.9	5454	−0.43	−16	0	164	4	30	12	191	11	5796	4908	7262	19	2.204	0.99
Machermo	1.9	5443	−0.26	−37	129	192	32	32	32	145	35	5447	5166	5808	–	1.714	0.00
Melung	11.4	5386	−0.69	−4	−215	217	3	13	5	144	36	5164	4950	5578	32	2.525	0.86
Nare	6.9	5368	−0.56	−12	−494	136	13	40	23	233	53	5482	4752	6476	25	0.964	0.97
Ngojumba	98.3	5496	−0.56	−1	−173	189	3	24	9	184	4	5824	4674	8067	26	2.158	1.32
Nuptse	8.8	5615	−0.18	−7	0	73	16	27	20	218	38	5823	4885	7754	35	2.146	0.57
Phunki	1.7	–	–	−5	−363	–	15	65	50	210	30	5465	4720	6553	–	0.204	0.00
Thyangbo	13.6	5139	–	−35	−72	210	22	40	33	129	51	5469	4335	6793	9	1.478	0.32
Tingbo	1.3	5271	−0.31	−13	−64	29	18	40	29	241	61	5440	4886	6090	40	0.589	0.00
Wlhotse	4.7	5280	−0.20	−5	−30	193	3	47	25	203	23	5742	4954	7649	37	2.803	0.29
Sum	360																
Median	5.8	5377	−0.45	−6	−121	189	9	40	23	179	39	5480	4861	6502	28	1.769	0.50
Mean	12.9	5345	−0.38	−13	−153	171	13	39	24	175	42	5522	4827	6745	27	1.755	0.54
Min	1.2	4969	−0.76	−56	−537	−2	3	13	5	77	4	5112	4335	5575	0	0.126	0.00
Max	98.3	5655	0.16	7	129	408	32	79	54	241	103	6163	5258	8467	66	3.023	2.07

density. Therefore, following the same methodological criteria described in Salerno et al. (2012), we manually digitized the surface area of supraglacial ponds even in 2011 using a Landsat ETM+ scene (Landsat-11, pixel 15 m) referred to the post monsoon season (30 November 2011, details on this scene in Thakuri et al., 2014). Fig. S2 of Supplementary Materials presents the extremely high agreement ($r = 0.94$, $p < 0.001$) between the supraglacial pond surface area of the two analysed post monsoon seasons. Therefore, the 2011 data will not be further discussed in the paper.

Thermal resistance of debris layer is defined as thickness divided by thermal conductivity (Nakawo and Young, 1982). It can be used as a proxy of debris thickness, as it was applied in some studies in the Himalayas (e.g., Suzuki et al., 2007; Zhang et al., 2011; Fujita and Sakai, 2014). Suzuki et al. (2007) proposed a method to calculate thermal resistance distribution from remotely sensed data and reanalysis data. In this study, thermal resistance (*Therm_resist*) is calculated with surface temperature and albedo data derived from Landsat satellite imagery, and downward shortwave and longwave radiation fluxes from the ERA-Interim reanalysis dataset. We calculate here the thermal resistance from four scenes of Landsat data, which are selected during the post-monsoon season from 2001 to 2016 (Table S1). The uncertainty related to the estimated thermal resistance was evaluated by comparing thermal resistance of each of four considered scenes (Fig. S3). Variability seems small (Fig. S3a) and the linear regression of standard deviation against the averaged thermal resistance indicates that the uncertainty is up to 0.02 $m^2\,K\,W^{-1}$, i.e., 6% (Fig. S3b). Final results for all considered glaciers are summarized in Fig. S4 and Table S2.

To explain the supraglacial pond distribution as a function of morphological predictors, glaciers were sub-divided into upstream and downstream zones distinguished on the basis of their slopes. For all considered glaciers, the upstream zones have steeper median surface gradients (40°) than the downstream ones (9°) (Table 1) (hereafter, these zones are called *Up_gradient and Down_gradient*, respectively). The criteria used for distinguishing the two areas was the change point of the glacier slope. To this end, they applied the CuSum (cumulative sum) control chart statistical technique (e.g., Taylor, 2000) to detect this change point in glacier slope along each glacier's longitudinal profile. The CuSum control chart is a sequential analysis technique used in various disciplines for performing change detection. It provides comparative information that can be useful in series analysis (in this case, the hypsographic curve) to identify potential changes in trend means (in this case, a change in glacier slopes).

In terms of glacier aspect, in order to linearize this circular variable (0°–360°), we calculated its absolute deviance from the south. Using this method, east- or west-facing glaciers have the same deviation (90°) from the south. Hereafter, this variable is termed *Mean_dev_from_south*.

3.1. Statistical analysis

All selected morphological parameters were tested for their ability to predict $\Delta Surf$, ΔSLA, $\Delta Term$, and $\Delta Elev$. The degree of correlation among the data was verified using correlation coefficients (r) after using a quantile-quantile plot of the model residuals to ensure that they followed a normal distribution. Otherwise, the data were log-transformed to meet the statistical requirements of the normal distribution; the residuals of the regressions were then tested for homoscedasticity (not shown here) (e.g., Venables and Ripley, 2002). All tests are implemented in the software R with a significance level of $p < 0.05$. The normality of the data is tested using the Shapiro–Wilk test (Shapiro and Wilk, 1965). The data were also tested for homogeneity of variance with Levene's test (Venables and Ripley, 2002).

We further derived simple multiple regression models considering only additions among all predictors, i.e., quadratic terms and interactions were not considered. The modelling was conducted using stepwise simplification through the evaluation of the AIC (Akaike Information Criterion) index. The AIC index (calculated using the "stepAIC" function from the MASS library in R) is a measure of the relative quality of statistical models for a given set of data. Given a collection of models for the data, AIC estimates the quality of each model relative to each of the other models. Hence, AIC provides a means for model selection: the smaller the AIC value is, the better the model will be (Akaike, 1974). At the end of the process, the hypothesis that the final model adds significant explanatory value over the model which considers only a single predictor was tested using an ANOVA F-test (Venables and Ripley, 2002). We used an information-theoretic approach, rather than one based on probability, because information criteria have several advantages for the type of multiple regression analysis performed here (Hector and Bagchi, 2007).

Moreover, we conducted a Principal Component Analysis (PCA) among the explanatory variables and predictors to obtain information on the relationships among the data and to summarize the reasons that could justify the observed changes (e.g., Salerno et al., 2014, 2016a, 2016b; Viviano et al., 2014). This analysis was performed by using the "princomp" and "biplot" functions in the R Project environment (e.g., Venables and Ripley, 2002).

4. Results

4.1. Description of data

The complete dataset considered in this analysis is presented in Table 1 for the period 1992–2008. The mean $\Delta Elev$ is -0.38 ± 0.20 $m\,a^{-1}$. Of interest is the wide range of observed changes; the change in surface elevation ranges from -0.76 to $+0.16$ $m\,a^{-1}$ and the change in surface area (which has an average of $-13 \pm 3\%$) ranges from -56% to $+1\%$ (Kdu_gr181 and Khumbu Glacier, respectively). Most of the glacier termini are stable over the 1992–2008 period, except for that of a small glacier (Kdu_gr38) that experienced a retreat of 537 m. High variability is also registered for the SLA, which ranges from -2 m for Kdu_gr125 to 408 m for the Bhotekhosi.

Considering the morphological boundary conditions treated in this study as potential predictors of glacier changes, we observed that, in this region, glaciers are south-facing (175°) on average, although some of them are predominantly east- (Kdu_gr38 and Cholo) and west- (Tingbo and Kdu_gr181) facing. The mean glacier surface gradient (*Mean_gradient*) is, as median, very steep (23°) but also very variable and ranges from 5° to 54°. A conspicuous difference is found in the median values of *Down_gradient* and *Up_gradient* (9° and 40°, respectively). In fact, it was always possible to find a clear change point between the steep upstream areas and the gently sloping downstream tongues of glaciers. Furthermore, even for these variables, the differences among glaciers are elevated. In this analysis, we also considered debris coverage, considering the current research interest on this topic. On average, the glaciers within the study region are on average 26% debris-covered, although there are 6 cases in which the debris coverage is less than 10%. The range of *Therm_resist*, computed here as a proxy of the debris thickness, is very wide: from 0.13 ± 0.08 for Kdu_gr181 Glacier to 3.02 ± 1 for Lobuche Glacier (10^{-2} $m^2\,K\,W^{-1}$).

4.2. Relationships among data

The main findings of this analysis are summarized in the correlation matrix shown in Fig. 2. Correlations are divided into four blocks to facilitate interpretation. The green rectangle shows the

	Δelev	*Δsurf*	*Δterm*	*ΔSLA*	*Down surface gradient*	*Up surface gradient*	*Mean surface gradient*	*Mean deviation from south*	*Min elevation*	*Mean elevation*	*Max elevation*	*Debris cover*	*Debris thickness*	*Pond density*	*SLA*	*Surf*
Δelev	1															
Δsurf	-0.63	1														
Δterm	0.05	0.54	1													
ΔSLA	-0.65	0.59	0.09	1												
Down surface gradient	0.70	-0.74	-0.26	-0.72	1											
Up surface gradient	0.60	-0.52	-0.26	-0.52	0.48	1										
Mean surface gradient	0.73	-0.79	-0.44	-0.60	0.78	0.80	1									
Mean deviation from south	0.57	-0.56	-0.50	0.36	0.66	0.43	0.71	1								
Min elevation	0.07	-0.25	0.30	0.16	-0.30	0.00	-0.15	-0.50	1							
Mean elevation	0.14	-0.06	0.07	0.05	-0.32	0.10	-0.09	-0.43	0.20	1						
Max elevation	-0.20	0.42	0.30	0.38	-0.40	-0.09	-0.23	-0.44	0.87	-0.07	1					
Debris cover	-0.44	0.60	0.41	0.32	-0.28	-0.14	-0.28	-0.14	-0.19	-0.16	-0.07	1				
Debris thickness	-0.36	0.35	0.38	0.46	-0.47	-0.36	-0.53	-0.51	0.10	0.06	0.35	0.18	1			
Pond density	-0.68	0.55	-0.02	0.58	-0.70	-0.55	-0.76	-0.39	0.06	0.02	0.24	0.04	0.37	1		
SLA	-0.47	0.37	0.19	0.28	-0.50	-0.48	-0.56	-0.71	0.67	0.49	0.54	0.15	0.26	0.46	1	
Surf	-0.58	0.64	0.20	0.68	-0.72	-0.63	-0.77	-0.63	0.51	0.06	0.62	-0.02	0.45	0.75	0.67	1

Legend

p<0.1	p<0.05	p<0.01	p<0.001

Fig. 2. Correlation matrix among all data considered in this study. Negative correlation coefficients mean inverse relationship. Acronyms are detailed in caption of Table 1. Correlations are divided into four blocks to facilitate interpretation. The green rectangle shows the mutual relationships among the morphological predictors. The orange rectangle points out the relationships among indicators of glacier state and all other considered variables. The red block highlights the mutual correlations among the selected indicators of glacier change. Finally, the blue block notes the dependence of each of the explanatory variables on the potential predictors. Glacier surface area (*Surf*) and terminus change (Δ*Term*) were log-normalized before inclusion in the statistical model. (For interpretation of the references to colour in this figure legend, the reader is referred to the web version of this article.)

mutual relationships among the morphological predictors. The orange rectangle shows the relationships among indicators of glacier state (*Surf*, the glacier surface area, and *SLA*, the snow line altitude in 1992) and all other considered variables. The red block shows the mutual correlations among the selected indicators of glacier change (i.e., the explanatory variables, Δ*Surf*, Δ*SLA*, Δ*Term*, and Δ*Elev*). Finally, to address the main purpose of this analysis, the blue block notes the dependence of each of the explanatory variables on the potential predictors.

The results are described below in two sections. First, in Sect. 4.2.1, we present the mutual relationships among the morphological characteristics (green block). In the same section, we describe how these features determine the glacier states (orange block). Afterwards (in Sect. 4.2.2), we describe how the morphological boundary conditions control the glacier changes (blue block) and the mutual relationships among the indicators of change (red block). All scatter plots related to Table 1 are presented in Fig. S5 of Supplementary Materials. Furthermore, in order to facilitate the interpretation of findings, results are summarized through the PCA discussed in Sect. 5.2.

4.2.1. Morphological characteristics of glaciers and their relationship with Surface area, SLA, Supraglacial pond density, Debris coverage, and Debris thickness

Surface gradient: the overall glacier surface gradient (*Mean_gradient*) is well correlated with both the downstream gradient (*Down_gradient*) ($r = 0.78$, $p < 0.001$) and with the upstream gradient (*Up_gradient*) ($r = 0.80$, $p < 0.001$), although between them the correlation is not so high ($r = 0.48$, $p < 0.05$).

Elevation: generally, the mean, min, and max glacier elevations (*Mean_elev, Min_elev, Max_elev*, respectively) do not present significant relationships with the other morphological variables. We note that south oriented glaciers (low values of *Mean_dev_from_south*) present mean terminus (*Min_elev*) located at higher elevation ($r = -0.50$, $p < 0.05$).

Aspect: glacier aspect (investigated here as mean deviation from south -*Mean_dev_from_south*-) is generally well correlated with the glacier surface gradients. Glaciers with an orientation deviating from south present steeper glacier surface gradients ($r = 0.71$, $p < 0.001$), and in particular, glaciers with these deviated expositions show higher *Down_gradient* than those glaciers presenting south orientations ($r = 0.66$, $p < 0.01$).

Surface area (*Surf*): Larger glaciers are more south oriented ($r = -0.63$, $p < 0.01$), presenting flatter downstream areas (*Down_gradient*) ($r = -0.72$, $p < 0.001$), higher elevations of *Min_elev* ($r = 0.51$, $p < 0.05$) and *Max_elev* ($r = 0.62$, $p < 0.01$).

Snow Line Altitude (*SLA*): Higher-elevation SLAs are found to be related mainly with gentler *Down_gradient* ($p = -0.50$, $p < 0.05$) and with glaciers more south oriented ($r = -0.71$, $p < 0.01$). The *SLA* is directly correlated also with *Mean_elev*, *Min_elev*, *Max_elev*, and in particular with the elevation of the terminus (*Min_elev*) ($r = 0.67$, $p < 0.01$).

Debris coverage (*Debr_cover*): The debris coverage does not present any significant relationship with the other morphological variables, in particular no relationship is found with the glacier altitudinal range and surface gradient. No relationship is found between *Debr_cover* and *Pond_dens*.

Debris thickness (*Therm_resist*): The thermal resistance, as a proxy of the debris thickness, presents a significant indirect relationship with the mean surface gradient *Mean_slope* ($r = 0.53$, $p < 0.05$), mainly with the downstream surface gradient ($r = 0.47$, $p < 0.10$). No relationship is found with the glacier altitudinal range, *Debr_cover* and *Pond_dens*.

Supraglacial pond density (*Pond_dens*). Supraglacial pond density is indirectly correlated with *Down_gradient* ($r = -0.70$, $p < 0.01$) and *Up_gradient* ($r = -0.55$, $p < 0.05$). Larger glaciers present higher *Pond_dens* ($r = 0.75$, $p < 0.001$).

4.2.2. Control of morphological boundary conditions on glacier changes

Terminus changes ($\Delta Term$): The main retreats are observable for glaciers located far from the south orientation ($r = -0.50$, $p < 0.05$).

Surface area changes ($\Delta Surf$): Larger surface area reduction occurred for glaciers located far from the south orientation ($r = -0.56$, $p < 0.05$) and for glaciers with higher *Down_gradient* ($r = -0.74$, $p < 0.001$). Reduced losses of surface area are observable for those glaciers with more debris *Debr_cover* ($r = 0.60$, $p < 0.01$) and where lower *Pond_dens* is developed ($r = 0.55$, $p < 0.05$). No relationship is found with thermal resistance.

Snow line altitude changes (ΔSLA): Higher upward shifts are observable for glaciers with lower *Down_gradient* ($r = -0.72$, $p < 0.001$) and on which higher *Pond_dens* is developed ($r = 0.58$, $p < 0.05$).

Elevation changes ($\Delta Elev$): At steeper glaciers we find less surface lowering ($r = 0.73$, $p < 0.001$). This dependence is higher considering specifically the downstream gradient, i.e., *Down_gradient* ($r = 0.70$, $p < 0.01$). South oriented glaciers present the greater surface lowering ($r = 0.57$, $p < 0.05$). A weak relationship is found with the *Debr_cover* ($r = -0.44$, $p < 0.1$), i.e., greater surface lowering is found for glaciers more covered by debris. However, no relationship is found with thermal resistance. More significant is the relationship between $\Delta Elev$ and *Pond_dens* ($r = -0.68$, $p < 0.01$), i.e., greater surface lowering is found for glaciers with higher supraglacial pond density.

Relationship among the indicators of glacier change: Glaciers showing greater surface lowering experienced larger upward shift of *SLA* ($r = -0.65$, $p < 0.01$), but less surface area shrinkage ($r = -0.63$, $p < 0.01$). On the contrary, greater surface area reductions correspond to less shift of *SLA* and greater terminus retreats ($r = 0.54$, $p < 0.05$).

5. Discussion

5.1. Morphological factors that control glacier features

Here we attempt to explain the findings described in Sect. 4.2.1. First, we observe that, as the aspect deviates from the south, the glaciers become significantly smaller and steeper. As an hypothesis, the reason could be found considering that these glaciers are located in valleys that are perpendicular to the prevailing south-north direction of the monsoon. These valleys could be less hollowed out by the precipitation-driven geomorphic processes. Thus, they contain steep terrain, and the glaciers in these valleys are subjected to greater driving stresses, which could favour loss of ice due to topographic instabilities (i.e., more frequent avalanches) (e.g., Bernhardt and Schulz, 2010). In contrast, south-oriented valleys (hereafter south-valleys) present gentle surface gradients that have been deeply excavated by the south Asian monsoon. Glaciers lying in these south-valleys (hereafter south-glaciers) are thus able to grow to larger sizes. In particular, we observed that the surface gradients of downstream valleys, which correspond to the surface gradients of the downstream areas of the glaciers, is the main favourable controlling factor for glacier surface development.

Large south-glaciers have fronts located at higher elevations than glaciers deviating from the south. This is probably due to the higher insolation occurring in the south-valleys, which likely receive more solar energy as a main heat source for glacier melting (Fujita and Ageta, 2000; Azam et al., 2012). Under these conditions, we also found glaciers with higher elevated SLAs.

In fact, we can say generally that, whereas elevation is a proxy for temperature (Salerno et al., 2008; Salerno et al., 2014; Racoviteanu et al., 2015), aspect is a proxy for insolation (Oliphant et al., 2003), and surface gradient is the key factor responsible for the transport of ice and rock from upstream to downstream glacier areas (Scherler et al., 2011a, 2011b). Considering that south-glaciers likely receive more solar radiation (Oliphant et al., 2003), the observed pattern of glacier sizes and their spatial distribution appears counterintuitive, but it can be justified that, on these glaciers, the driving stresses (conditioned by surface gradients) are the key factor in determining glacier size, while the SLA elevation is governed by the glacier aspect, which controls the quantity of insulation and thus the heat balance on the glacier surface.

Debris coverage did not show any significant relationship with the other morphological variables, while its thickness (thermal resistance) is higher for gentle downstream surface gradients. We suppose that reduced downstream surface gradients could favour the accumulation of debris. Moreover, we found a significant relationship between debris thickness and glacier aspect, i.e., south oriented glaciers presents higher debris thicknesses. Even in this case this relationship could be explained considering that glacier are more gentle at these orientations. However, in this regard, Nagai et al. (2013) argued that the SW-facing upper slope situated above the glacier could supply more debris through the enhanced diurnal freeze–thaw cycles, which could favour permafrost degradation and snow avalanches.

Supraglacial pond density is found to be larger for glaciers with gently sloping lower and upper regions. As previously described in Salerno et al. (2012), the model that considers the surface gradients of the two glacier areas separately is able to describe the supraglacial pond surfaces better than the model considering the mean surface gradient of the glacier as a whole. In this regard, many studies have shown that the present condition of ice stagnation of glaciers in the southern central Himalayas is attributable to the low flow velocities generated by generally negative mass balances. An increase in glacier flow can be attributed to an increase in the glacier surface gradient brought on by an imbalance between the amounts of accumulation versus ablation. This imbalance increases the shear stress on a glacier until it begins to flow. The greater the upstream glacier surface gradient, the greater the possibility that an addition of new snow and ice will be transferred to the lower zone, and therefore the higher the flow velocity of the glacier terminus is expected to be. Therefore, given two glaciers, the one with a more gently sloping upstream region presents more favourable conditions for the development of supraglacial ponds caused by a minor transport of new snow and ice, which decreases the flow velocity of the glacier termini.

5.2. Morphological controlling factors for glacier changes

Now that we have described the "morphological boundary system" in the previous section, we now attempt to rationalize the correlations shown in Sect. 4.2.2. First, we discuss one of the main findings of this analysis that is related to glacier elevation change. We observed that glaciers react to the same climatic forcing in different ways, i.e., along a spectrum with one extreme involving significant surface lowering and high upward shift of *SLA*, and the other involving large surface area reduction and terminus retreat. The main morphological controlling factor of this behaviour

Table 2
Linear multi regression equations between morphological control factors (*Up_gradient*/*Down_gradient*: surface gradient of upstream, downstream glacier; *Pond_dens*: supraglacial pond density; *Debr_cover*: debris coverage; *Therm_resist*: thermal resistance as a proxy of debris thickness; *Mean_dev_from_south*: glacier orientation). In the table the regression coefficients are reported, all terms were found significant at $p < 0.05$.

Predictors	Explanatory variables			
	$\Delta Elev$ ($\mathrm{m\,a^{-1}}$)	ΔSLA (m)	$\Delta Surf$ (%)	$\Delta Term$ (m)
Intercept	−0.44	181	−0.10	−2.15
Down_gradient (°)	0.02	−4.9	−0.001	–
Up_gradient (°)	–	–	–	–
Pond_dens ($\mathrm{km^2/km^2}$)	−0.18	290	–	–
Debr_cover (%)	–	–	0.003	–
Therm_resist ($\mathrm{m^2\,K\,W^{-1}}$)	–	–	–	–
Mean_dev_from_south (°)	–	–	–	−63.1

is the glacier surface gradient and in particular the surface gradient of the downstream portion of the glacier. Glaciers presenting downstream areas with gentle surface gradients (mainly south-glaciers) present the greatest surface lowering, high upwards shift of *SLA*, limited surface area losses and terminus retreats. Two examples of these extremes are shown in Fig. 4: glaciers that exemplify this pattern include Lhotse (Fig. 4, on the left), Bhotekhosi, and Melung (from Table 1, the mean values for these glaciers are *Down_gradient* = 3.9°, *Mean_aspect* = 175°, *Mean_dev_from_south* = 5°, $\Delta Elev = -0.70\ \mathrm{m\,a^{-1}}$, $\Delta SLA = 292$ m, $\Delta Surf = -2.6\%$, and $\Delta Term = -230$ m). In contrast, steeper glaciers, which deviate from south-valleys, present opposite changes: large losses of surface area and higher front retreats, but the lowest surface lowering and reduced upwards shift of *SLA*. Glaciers that exemplify this pattern are Cholo (Fig. 4, on the right), Kdu_gr38, and Langmuce (from Table 1, the mean values for these glaciers are *Down_gradient* = 24.3°, *Mean_dev_from_south* = 95°, $\Delta Elev = +0.02\ \mathrm{m\,a^{-1}}$; $\Delta SLA = 98$ m, $\Delta Surf = -30.3\%$, and $\Delta Term = -292$ m). Elevation profiles, related to the two proposed examples shown in Fig. 4, are presented in Fig. 5.

Further, to investigate possible additive properties between factors controlling these glacier changes, we derived multiple regression models. The process of models development was conducted by stepwise simplification through the evaluation of the AIC index. We present here just the final step of the process, which is the result considering both the highest quality of the fit and the lowest number of equation terms (Akaike, 1974; Venables and Ripley, 2002; Hector and Bagchi, 2007; Salerno et al., 2012). Many variables were excluded from the final setting because their contribution did not appear to be significant in improving the predictive ability of the model. Table 2 shows the significant factors controlling the glacier changes. *Down_gradient* and *Pond_dens* together generate a model with a performance that is significant and greater than the ability of any individual variable in predicting $\Delta Elev$ and ΔSLA ($r = 0.78$, $p < 0.001$; $r = 0.79$, $p < 0.001$, respectively). For these explanatory variables, *Debr_cover* is not a significant controlling factor, while the contribution of *Debr_cover* is significant (over *Down_gradient*) in explaining $\Delta Surf$ ($r = 0.74$, $p < 0.001$).

How can we interpret the results of the simple (Fig. 2) and multiple (Table 2) regression analyses?

With regard to the loss of surface area, surface gradient as a morphological factor controlling glacier shrinkage has been previously observed by Salerno et al. (2014), Loibl et al. (2014) and Racoviteanu et al. (2015). These authors support the idea that driving stresses favour detachment and loss of ice blocks. However, we observe here that a high debris coverage seems to protect glaciers from losses, perhaps because, as an hypothesis ice that includes debris is more compact and less subject to detachment.

Turning to the changes in glacier elevation, from a physical point of view, lower surface gradients are thought to induce reduced glacier ice flow, thus allowing the development of stagnant ice (e.g., Scherler et al., 2011a). Under these conditions, consequent lower terminus retreat rates have already been observed (Scherler et al., 2011a; Bolch et al., 2008), as well as the development of supraglacial ponds (Salerno et al., 2012; Thakuri et al., 2016; Ragettli et al., 2016). In this analysis, we note that downstream surface gradients over 15° inhibit glacier surface lowering, while the greatest surface lowering is found on downstream surface gradients lower than 5° (Fig. 4). Therefore, the lower glacier velocity induced by gentler surface gradients, which produce stagnant conditions, is also responsible for greater downwasting. Moreover, we show that higher supraglacial pond density is a further significant and negative controlling factor on glacier elevation change, i.e., greater surface lowering is found for glaciers with higher supraglacial pond density. Although there is some auto-correlation among these variables, the supraglacial pond density is found to be a significant predictor in the multiple regression model, which means that the pond density is an independent and additional factor that controls glacier elevation change. Gently sloping glacier downstream areas favour both higher surface lowering and the development of supraglacial ponds, but where supraglacial ponds are able to develop (i.e., for glaciers that also have gently sloping upstream areas), the glaciers register additional surface lowering.

Moreover, we observe that the additional control exercised by supraglacial ponds is also significant in determining changes in SLA. This relationship is because a correspondence between greater surface lowering and larger upward shifts of *SLA* has been observed. Therefore, our finding that shifts in SLA are a good predictor of glacier mass balance indicates that they are related to the same morphological factors controlling changes in glacier surface elevation.

This analysis thus confirms the hypothesis of those authors who consider that supraglacial ponds enhance the melt of debris-covered ice by absorbing radiative heat as hot spots (Sakai et al., 2000, 2002; Buri et al., 2015; Miles et al., 2016), such that their distribution and density are important for better understanding the mechanisms of glacier degradation. Lamsal et al. (2016) recently found a significant negative correlation between the size of supraglacial ponds and the rate of elevation change, indicating that at sites where larger supraglacial ponds exist, the glacier surface is more down-wasted than at sites where smaller ponds exist. This observation was explained based on the consideration that the energy absorption by supraglacial ponds is several times larger than that of the surrounding debris-covered surface (Sakai et al., 2000; Miles et al., 2016).

This analysis concludes with the PCA of Fig. 3, which provides an overall overview of the mutual relationships among the selected explanatory variables and the main controlling factors considered in this work. The bottom and left axes represent the "scores" of the analysis. We observe that the first principal component (PC1) explains 57% of the variance, while the second one (PC2) explains 26%. The top and right axes show the "factor loadings". The black points represent the positions of glaciers with reference to the first pair of axes, while the lengths of the arrows refer to the second factor loadings. Factor loadings, representing the weightings of variables into each component, are the key to understanding the underlying nature of a particular factor. Red labels represent the main explanatory variables, while the green ones represent the main morphological factors identified from the cross-correlation matrix shown in Fig. 2. To simplifying the reading of the PCA, we do not consider in this figure the relative change (Δ) of the explanatory variables, but, we use the surface lowering, surface area loss, terminus retreat and upward shift in the SLA directly. The green ellipse represents the 95% confidence interval for the data:

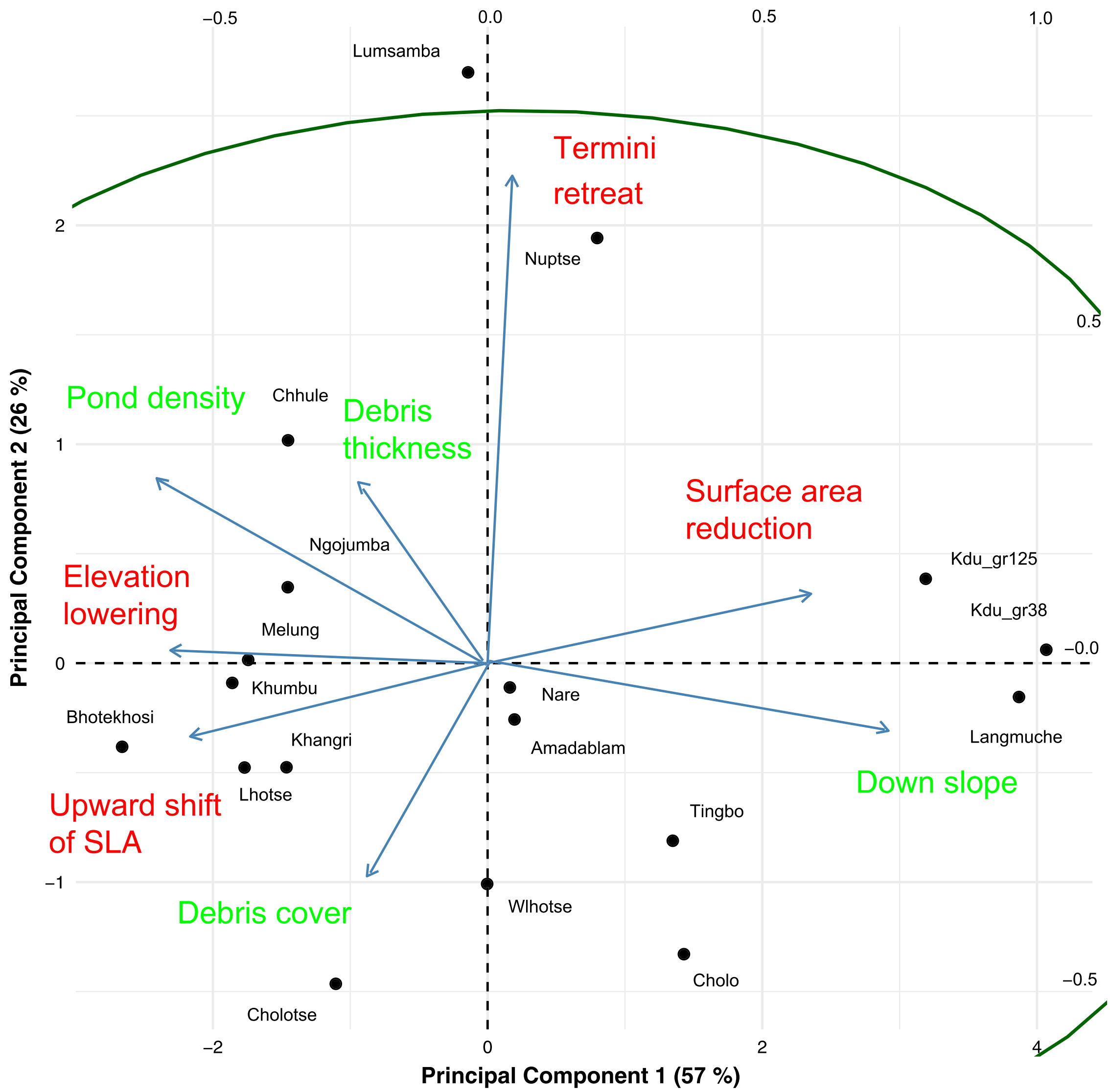

Fig. 3. Summary of results: PCA among glacier changes (red labels) and main morphological predictors (green labels). The green ellipse represents the 95% confidence interval for data. Refer to the text for details on this figure. (For interpretation of the references to colour in this figure legend, the reader is referred to the web version of this article.)

there is only one outlier (Lumbsamba Glacier). This means that data analysed are normally distributed and that the relationships described in this study characterize quite all considered glaciers. In PC1, the variables with positive loadings are the surface area reduction and the downstream surface gradient; all the others have negative loadings. Therefore the PCA helps us to simplify the relationships described in this study: when the arrows point in the same direction the relationships are direct, on the contrary are indirect.

6. Conclusions

There is presently an open debate on the thinning rates of debris-covered glaciers. Some authors defend the more classic idea, which considers that the insulating effect of debris covers has a larger effect on total mass loss than the enhanced ice ablation due to supraglacial ponds and exposed ice cliffs. In contrast, other studies have observed similar rates as those seen on clean glaciers and hypothesize that these glacial features may act as a catalyst for melting by absorbing radiative heat as hot spots. This similarity is recently referred as the "debris-covered glacier anomaly".

So far, previous studies have adopted a deterministic approach, which is indispensable but mainly based on laborious field campaigns. Considering the remoteness of the region, only a few glaciers could be monitored using these methods. In some cases, the necessary observations were not performed at the spatial scale of an entire glacier, and indeed, were limited to areas around the relevant glacial features. This is because supraglacial ponds and ice cliffs are small-scale features on the glacier surface and thus require high-resolution (e.g., in situ) observations.

In this context, the analysis proposed here, which is based on a larger population of glaciers, is not an alternative, but a complement to these deterministic studies. The proposed stochastic approach was not able to directly represent the physical processes, but at the same time was able to identify strong possibilities for relationships among the selected indicators of glacier change and morphological factors. However, it is often emphasized in statistics that a correlation between two variables does not necessarily imply that one variable causes the other (e.g., Aldrich, 1995).

We analysed 28 glaciers lying on the southern slopes of Mt. Everest (central southern Himalaya) during the period 1992–2008. This was made possible by combining data referring to the same glaciers during the same period and derived from three recent

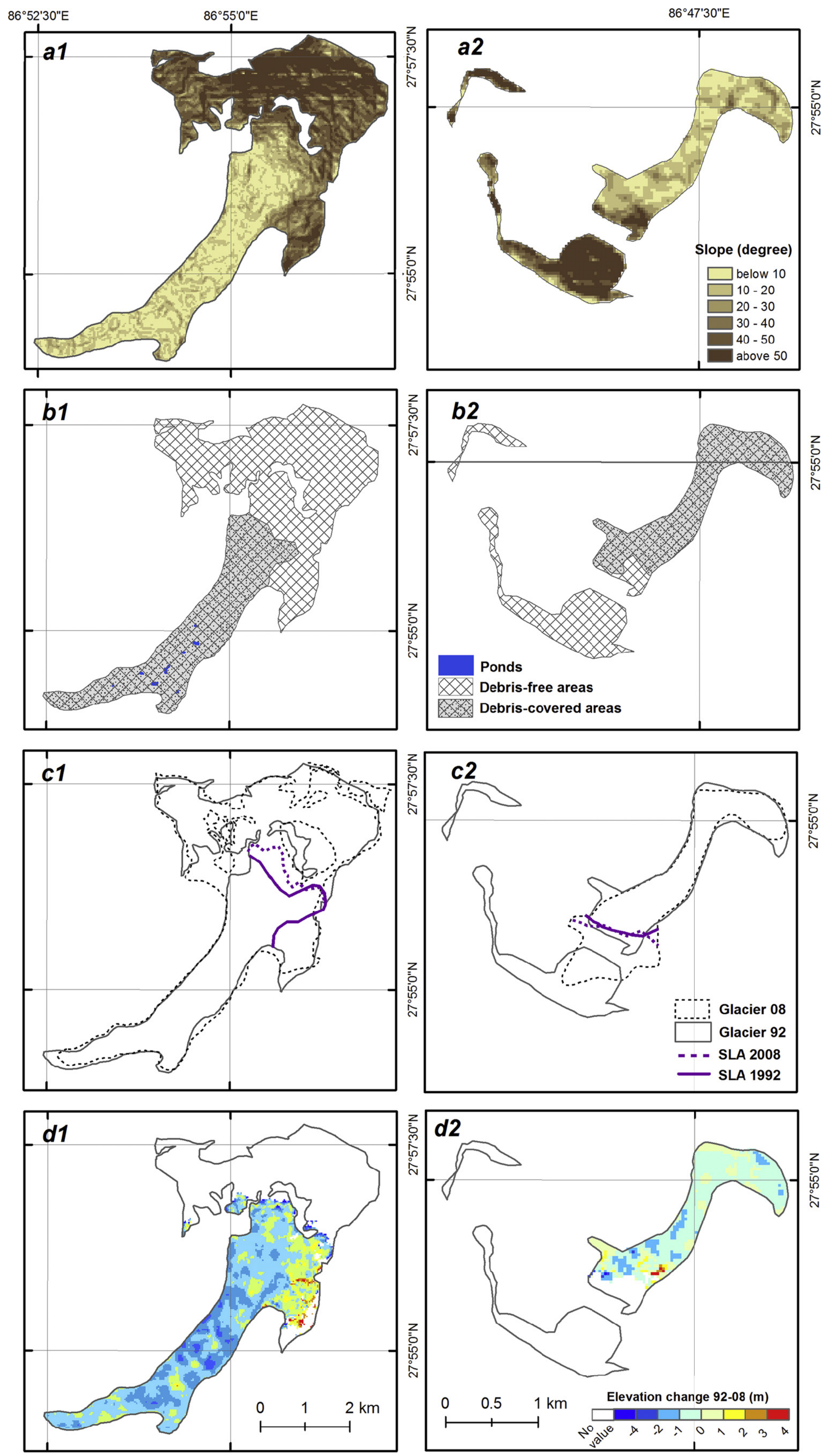

Fig. 4. Examples of opposite changes occurred for two glaciers in SNP: on the left the Lhotse Glacier; on the right the Cholo Glacier. For both glaciers: a) glacier slope derived from DEM; b) debris coverage and supraglacial ponds; c) changes in surface area, SLA, and terminus position; changes in elevation; d) glacier elevation change. Glaciers presenting downstream areas with gentle surface gradients, mainly south-glaciers, as the case shown in this figure of Lhotse Glacier, show the highest supraglacial pond density, the greatest surface lowering, high upwards shift of SLA and limited surface area losses.

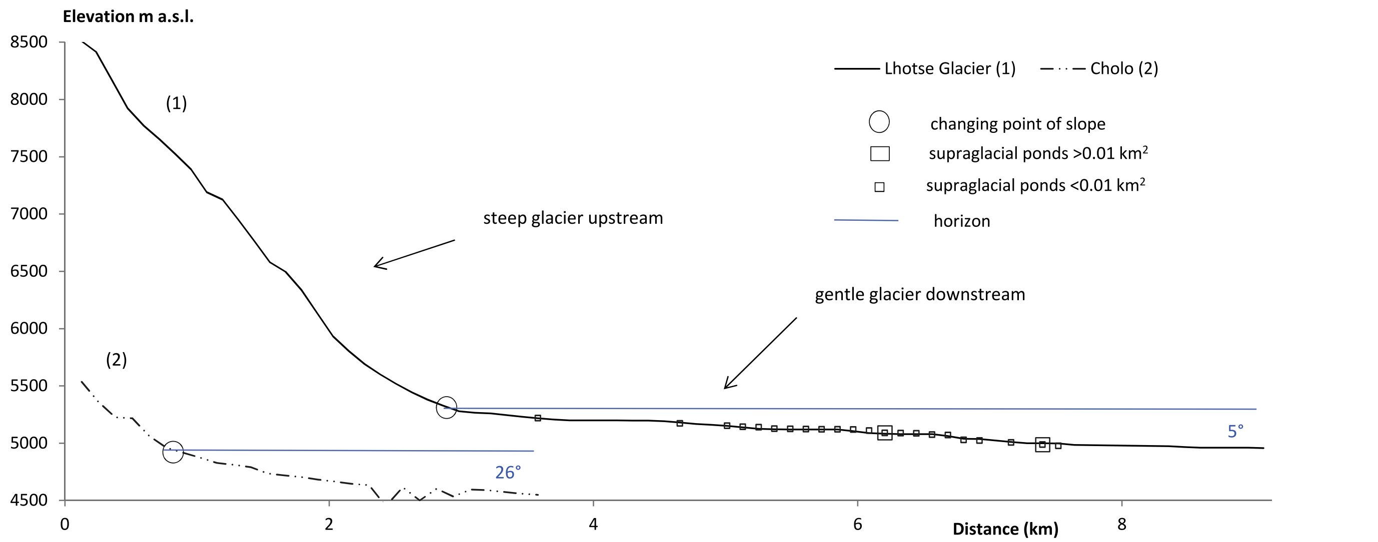

Fig. 5. Elevation profiles related to the two proposed examples in Fig. 4: Lhotse Glacier and Cholo Glacier. The location of the change in slope (derived from DEM) is indicated, and supraglacial pond locations in 2008 are shown from Salerno et al. (2012).

published works (Nuimura et al., 2012; Salerno et al., 2012; Thakuri et al., 2014) in a unique statistical analysis. It was possible to answer the question we posed here:

"What are the main morphological factors controlling the observed heterogeneous responses of debris-covered glaciers to climate change in the southern central Himalaya?"

The following key points emerged from the analysis carried out here and are therefore valid for this geographical and temporal context:

1) South-facing valleys have gentle surface gradients because they have been deeply excavated by the south Asian monsoon. Glaciers within these valleys are able to grow to larger sizes. We observed a clear spatial pattern regulating the glacier responses to climate change: south-facing glaciers, which have flatter downstream areas, tend to be more subject to lowering of the glacier surface, to developing supraglacial ponds and to shift their SLAs upwards. Glaciers deviating from the south orientation, which are steeper, tend to lose more surface area and their termini retreat.
2) Larger glaciers experienced high rates of surface lowering and upward shifts of their SLAs, corresponding to slight surface area reductions and retreats of their termini. Therefore, elevation change is the best indicator in this region to describe the responses of glaciers to climate change and the shift of SLA can be used as suitable proxy to describe this impact, as the two variables directly correlated.
3) Considering that the climatic forcing in this region is homogeneous, the changes observed in the glacier responses are indeed heterogeneous. We have shown that the differences are mainly due to glacier surface gradients. Previous studies have demonstrated that flatter downstream and upstream areas favour the development of supraglacial ponds. We found here that the downstream surface gradient is also responsible for higher glacier elevation lowering. This morphological factor controls ice flow velocity: gentle surface gradients, which produce low velocities and possibly stagnant conditions that favour the development of supraglacial ponds and elevation lowering.
4) The development of supraglacial ponds was found here to be a further controlling factor of glacier elevation change. Where supraglacial ponds are able to develop (i.e., for glaciers that have gently sloping upstream areas), glaciers display further surface lowering. This analysis thus confirms the hypothesis of those authors who consider that supraglacial ponds enhance the melting of debris-covered ice.
5) The debris coverage and thickness were not found to be significantly responsible for the development of supraglacial ponds, the elevation changes, or the shift in SLAs. On the other hand, reduced losses of surface area are observable for those glaciers with more debris coverage. Moreover, it does not present any significant relationship with the other morphological variables, in particular no relationship is found with the glacier altitudinal range, while the debris thickness is higher for gentle downstream surface gradients. We suppose that reduced downstream surface gradients could favour the accumulation of debris.

One important limit of the present study is related to unavailability of data on ice cliffs located on the analysed glaciers. In fact, these glacier forms are considered by some authors (e.g., Sakai et al., 2000, 2002; Buri et al., 2015; Miles et al., 2016; Thompson et al., 2016), as discussed here only for supraglacial ponds, important catalysts for melt and in particular in terms of mass loss (e.g., Thompson et al., 2016). We hope future studies could fill this gap.

Funding

This research did not receive any specific grant from funding agencies in the public, commercial, or not-for-profit sectors.

Appendix A. Supplementary material

Supplementary material related to this article can be found online at http://dx.doi.org/10.1016/j.epsl.2017.04.039.

References

Akaike, H., 1974. A new look at statistical model identification. IEEE Trans. Autom. Control 19, 716–723.

Aldrich, J., 1995. Correlations genuine and spurious in Pearson and Yule. Stat. Sci. 10, 364–376. http://dx.doi.org/10.1214/ss/1177009870.

Amatya, L.K., Cuccillato, E., Haack, B., Shadie, P., Sattar, N., Bajracharya, B., Shrestha, B., Caroli, P., Panzeri, D., Basani, M., Schommer, B., Flury, B., Manfredi, E.C., Salerno, F., 2010. Improving communication for management of social-ecological systems in high mountain areas. Mt. Res. Dev. 30, 69–79. http://dx.doi.org/10.1659/MRD-JOURNAL-D-09-00084.1.

Azam, M.F., Wagnon, P., Ramanathan, A.L., Vincent, C., Sharma, P., Arnaud, Y., Linda, A., Pottakkal, J.G., Chevallier, P., Singh, V.B., Berthier, E., 2012. From balance to imbalance: a shift in the dynamic behaviour of Chhota Shigri Glacier (Western Himalaya, India). J. Glaciol. 58, 315–324. http://dx.doi.org/10.3189/2012JoG11J123.

Bernhardt, M., Schulz, K., 2010. Snow Slide: a simple routine for calculating gravitational snow transport. Geophys. Res. Lett. 37, L11502. http://dx.doi.org/10.1029/2010GL043086.

Bolch, T., Buchroithner, M., Pieczonka, T., Kunert, A., 2008. Planimetric and volumetric glacier changes in the Khumbu Himal, Nepal, since 1962 using Corona, Landsat TM and ASTER data. J. Glaciol. 54, 592–600. https://doi.org/10.3189/002214308786570782.

Bolch, T., Kulkarni, A., Kääb, A., Huggel, C., Paul, F., Cogley, G., Frey, H., Kargel, J.S., Fujita, K., Scheel, M., Bajracharya, S., Stoffel, M., 2012. The state and fate of Himalayan glaciers. Science 336, 310–314. http://dx.doi.org/10.1126/science.1215828.

Bolch, T., Pieczonka, T., Benn, D.I., 2011. Multi-decadal mass loss of glaciers in the Everest area (Nepal Himalaya) derived from stereo imagery. Cryosphere 5, 349–358. http://dx.doi.org/10.5194/tc-5-349-2011.

Buri, P., Pellicciotti, F., Steiner, J., Miles, E.S., Immerzeel, W.W., 2015. A grid-based model of backwasting of supraglacial ice cliffs on debris-covered glaciers. Ann. Glaciol. 57, 199–211. http://dx.doi.org/10.3189/2016AoG71A059.

Fujita, K., Ageta, Y., 2000. Effect of summer accumulation on glacier mass balance on the Tibetan Plateau revealed by mass-balance model. J. Glaciol. 46, 244–252. http://dx.doi.org/10.3189/172756500781832945.

Fujita, K., Nuimura, T., 2011. Spatially heterogeneous wastage of Himalayan glaciers. Proc. Natl. Acad. Sci. USA 108, 14011–14014. http://dx.doi.org/10.1073/pnas.1106242108.

Fujita, K., Sakai, A., 2014. Modelling runoff from a Himalayan debris-covered glacier. Hydrol. Earth Syst. Sci. 18, 2679–2694. http://dx.doi.org/10.5194/hess-18-2679-2014.

Fujita, K., Suzuki, R., Nuimura, T., Sakai, A., 2008. Performance of ASTER and SRTM DEMs, and their potential for assessing glacial lakes in the Lunana region, Bhutan Himalaya. J. Glaciol. 54, 220–228. http://doi.org/10.3189/002214308784886162.

Gardelle, J., Arnaud, Y., Berthier, E., 2011. Contrasted evolution of glacial lakes along the Hindu Kush Himalaya mountain range between 1990 and 2009. Glob. Planet. Change 75, 47–55. http://dx.doi.org/10.1016/j.gloplacha.2010.10.003.

Hambrey, M.J., Quincey, D.J., Glasser, N.F., Reynolds, J.M., Richardson, S.J., Clemmens, S., 2008. Sedimentological, geomorphological, and dynamic context of debris-mantled glaciers, Mount Everest (Sagarmatha) region, Nepal. Quat. Sci. Rev. 27, 2361–2389. http://dx.doi.org/10.1016/j.quascirev.2008.08.010.

Hector, A., Bagchi, R., 2007. Biodiversity and ecosystem multifunctionality. Nature 448, 188–190. http://dx.doi.org/10.1038/nature05947.

Kääb, A., Berthier, E., Nuth, C., Gardelle, J., Arnaud, Y., 2012. Contrasting patterns of early twenty-first-century glacier mass change in the Himalayas. Nature 488, 495–498. http://dx.doi.org/10.1038/nature11324.

Kirkbride, M.P., Deline, P., 2013. The formation of supraglacial debris covers by primary dispersal from transverse englacial debris bands. Earth Surf. Process. Landf. 38, 1779–1792. http://dx.doi.org/10.1002/esp.3416.

Lamsal, D., Fujita, K., Sakai, A., 2016. Moderate mass loss of Kanchenjunga Glacier in the eastern Nepal Himalaya since 1975 revealed by Hexagon KH-9 and ALOS satellite imageries. Cryosphere Discuss. http://dx.doi.org/10.5194/tc-2016-202.

Loibl, D.M., Lehmkuhl, F., Grießinger, J., 2014. Reconstructing glacier retreat since the Little Ice Age in SE Tibet by glacier mapping and equilibrium line altitude calculation. Geomorphology 214, 22–39. http://dx.doi.org/10.1016/j.geomorph.2014.03.018.

Miles, E.S., Willis, I.C., Arnold, N.S., Steiner, J.F., Pellicciotti, F., 2017. Spatial, seasonal, and interannual variability of supraglacial ponds in the Langtang Valley of Nepal, 1999 to 2013. J. Glaciol. 63, 88–105. http://dx.doi.org/10.1017/jog.2016.120.

Miles, E.S., Willis, I., Pellicciotti, F., Steiner, J.F., Buri, P., Arnold, N., 2016. Refined energy-balance modelling of a supraglacial pond, Langtang Khola, Nepal. Ann. Glaciol. 57. http://dx.doi.org/10.3189/2016AoG71A421.

Nagai, H., Fujita, K., Nuimura, T., Sakai, A., 2013. Southwest-facing slopes control the formation of debris-covered glaciers in the Bhutan Himalaya. Cryosphere 7, 1303–1314. http://dx.doi.org/10.5194/tc-7-1303-2013.

Nakawo, M., Young, G.J., 1982. Estimate of glacier ablation under a debris layer from surface temperature and meteorological variables. J. Glaciol. 28, 29–34. http://dx.doi.org/10.1017/S002214300001176X.

Nuimura, T., Fujita, K., Yamaguchi, S., Sharma, R.R., 2012. Elevation changes of glaciers revealed by multitemporal digital elevation models calibrated by GPS survey in the Khumbu region, Nepal Himalaya, 1992–2008. J. Glaciol. 58, 648–656. http://dx.doi.org/10.3189/2012JoG11J061.

Oliphant, A.J., Spronken-Smith, R.A., Sturman, A.P., Owens, I.F., 2003. Spatial variability of surface radiation fluxes in mountainous region. J. Appl. Meteorol. 42, 113–128. http://dx.doi.org/10.1175/1520-0450(2003)042<0113:SVOSRF>2.0.CO;2.

Paul, F., Huggel, C., Kääb, A., 2004. Combining satellite multispectral image data and a digital elevation model for mapping debris covered glaciers. Remote Sens. Environ. 89, 510–518. http://dx.doi.org/10.1016/j.rse.2003.11.007.

Pellicciotti, F., Stephan, C., Miles, E., Herreid, S., Immerzeel, W.W., Bolch, T., 2015. Mass-balance changes of the debris-covered glaciers in the Langtang Himal, Nepal, from 1974 to 1999. J. Glaciol. 61, 373–386. http://dx.doi.org/10.3189/2015JoG13J237.

Pelto, M., 2011. Utility of late summer transient snowline migration rate on Taku Glacier, Alaska. Cryosphere 5, 1127–1133. http://dx.doi.org/10.5194/tc-5-1127-2011.

Quincey, D.J., Richardson, S.D., Luckman, A., Lucas, R.M., Reynolds, J.M., Hambrey, M.J., Glasser, N.F., 2007. Early recognition of glacial lake hazards in the Himalaya using remote sensing datasets. Glob. Planet. Change 56, 137–152. http://dx.doi.org/10.1016/j.gloplacha.2006.07.013.

Racoviteanu, A.E., Arnaud, Y., Williams, M.W., Manley, W.F., 2015. Spatial patterns in glacier characteristics and area changes from 1962 to 2006 in the Kanchenjunga–Sikkim area, eastern Himalaya. Cryosphere 9, 505–523. http://dx.doi.org/10.5194/tc-9-505-2015.

Ragettli, S., Bolch, T., Pellicciotti, F., 2016. Heterogeneous glacier thinning patterns over the last 40 years in Langtang Himal, Nepal. Cryosphere 10, 2075–2097. http://dx.doi.org/10.5194/tc-10-2075-2016.

Ragettli, S., Pellicciotti, F., Immerzeel, W.W., Miles, E.S., Petersen, L., Heynen, M., Shea, J.M., Stumm, D., Joshi, S., Shrestha, A., 2015. Unraveling the hydrology of a Himalayan basin through integration of high resolution in situ data and remote sensing with an advanced simulation model. Adv. Water Resour. 78, 94–111. http://dx.doi.org/10.1016/j.advwatres.2015.01.013.

Rowan, A.V., Egholm, D.L., Quincey, D.J., Glasser, N.F., 2015. Modelling the feedbacks between mass balance, ice flow and debris transport to predict the response to climate change of debriscovered glaciers in the Himalaya. Earth Planet. Sci. Lett. 430, 427–438. http://dx.doi.org/10.1016/j.epsl.2015.09.004.

Sakai, A., Nakawo, M., Fujita, K., 2002. Distribution characteristics and energy balance of ice cliffs on debris-covered glaciers, Nepal Himalaya. Arct. Antarct. Alp. Res. 34, 12–19. http://dx.doi.org/10.2307/1552503.

Sakai, A., Takeuchi, N., Fujita, K., Nakawo, M., 2000. Role of supraglacial ponds in the ablation process of a debris-covered glacier in the Nepal Himalayas. IAHS Publ. 264, 119–132.

Salerno, F., Buraschi, E., Bruccoleri, G., Tartari, G., Smiraglia, C., 2008. Glacier surface-area changes in Sagarmatha national park, Nepal, in the second half of the 20th century, by comparison of historical maps. J. Glaciol. 54, 738–752. http://dx.doi.org/10.3189/002214308786570926.

Salerno, F., Gambelli, S., Viviano, G., Thakuri, S., Guyennon, N., D'Agata, C., Diolaiuti, G., Smiraglia, C., Stefani, F., Bocchiola, D., Tartari, G., 2014. High alpine ponds shift upwards as average temperatures increase: a case study of the Ortles-Cevedale mountain group (Southern Alps, Italy) over the last 50 years. Glob. Planet. Change 120, 81–91. http://dx.doi.org/10.1016/j.gloplacha.2014.06.003.

Salerno, F., Guyennon, N., Thakuri, S., Viviano, G., Romano, E., Vuillermoz, E., Cristofanelli, P., Stocchi, P., Agrillo, G., Ma, Y., Tartari, G., 2015. Weak precipitation, warm winters and springs impact glaciers of south slopes of Mt. Everest (central Himalaya) in the last 2 decades (1994–2013). Cryosphere 9. http://dx.doi.org/10.5194/tc-9-1229-2015.

Salerno, F., Rogora, M., Balestrini, R., Lami, A., Tartari, G.A., Thakuri, S., Godone, D., Freppaz, M., Tartari, G., 2016a. Glacier melting increases the solute concentrations of Himalayan glacial lakes. Environ. Sci. Technol. 50, 9150–9160. http://dx.doi.org/10.1021/acs.est.6b02735.

Salerno, F., Thakuri, S., D'Agata, C., Smiraglia, C., Manfredi, E.C., Viviano, G., Tartari, G., 2012. Glacial lake distribution in the Mount Everest region: uncertainty of measurement and conditions of formation. Glob. Planet. Change, 92–93. http://dx.doi.org/10.1016/j.gloplacha.2012.04.001.

Salerno, F., Thakuri, S., Guyennon, N., Viviano, G., Tartari, G., 2016b. Glacier melting and precipitation trends detected by surface area changes in Himalayan ponds. Cryosphere 10, 1433–1448. http://dx.doi.org/10.5194/tc-10-1433-2016.

Scherler, D., Bookhagen, B., Strecker, M.R., 2011a. Spatially variable response of Himalayan glaciers to climate change affected by debris cover. Nat. Geosci. 4, 156–159. http://dx.doi.org/10.1038/ngeo1068.

Scherler, D., Bookhagen, B., Strecker, M.R., 2011b. Hillslope-glacier coupling: the interplay of topography and glacial dynamics in High Asia. J. Geophys. Res. 116, F02019. http://dx.doi.org/10.1029/2010JF001751.

Shapiro, S.S., Wilk, M.B., 1965. An analysis of variance test for normality (complete samples). Biometrika 52, 591–611.

Soncini, A., Bocchiola, D., Confortola, G., Minora, U., Vuillermoz, E., Salerno, F., Viviano, G., Shrestha, D., Senese, A., Smiraglia, C., Diolaiuti, G., 2016. Future hydrological regimes and glacier cover in the Everest region: the case study of the upper Dudh Koshi basin. Sci. Total Environ. 565. http://dx.doi.org/10.1016/j.scitotenv.2016.05.138.

Suzuki, R., Fujita, K., Ageta, Y., 2007. Spatial distribution of thermal properties on debris-covered glaciers in the Himalayas derived from ASTER data. Bull. Glaciol. Res. 24, 13–22.

Tartari, G., Salerno, F., Buraschi, E., Bruccoleri, G., Smiraglia, C., 2008. Lake surface area variations in the North-Eastern sector of Sagarmatha National Park (Nepal) at the end of the 20th Century by comparison of historical maps. J. Limnol. 67, 139–154. http://dx.doi.org/10.4081/jlimnol.2008.139.

Taylor, W.A., 2000. Change-Point Analysis: A Powerful New Tool For Detecting Changes. http://www.variation.com/cpa/tech/changepoint.html.

Thakuri, S., Salerno, F., Bolch, T., Guyennon, N., Tartari, G., 2016. Factors controlling the accelerated expansion of Imja Lake, Mount Everest region. Ann. Glaciol. 57. http://dx.doi.org/10.3189/2016AoG71A063.

Thakuri, S., Salerno, F., Smiraglia, C., Bolch, T., D'Agata, C., Viviano, G., Tartari, G., 2014. Tracing glacier changes since the 1960s on the south slope of Mt. Everest (central Southern Himalaya) using optical satellite imagery. Cryosphere 8. http://dx.doi.org/10.5194/tc-8-1297-2014.

Thompson, S., Benn, D.I., Mertes, J., Luckman, A., 2016. Stagnation and mass loss on a Himalayan debris-covered glacier: processes, patterns and rates. J. Glaciol. 62 (233), 467–485. http://doi.org/10.1017/jog.2016.37.

Venables, W.N., Ripley, B.D., 2002. Modern Applied Statistics with S. Springer, New York.

Vincent, C., Wagnon, P., Shea, J.M., Immerzeel, W.W., Kraaijenbrink, P., Shrestha, D., Soruco, A., Arnaud, Y., Brun, F., Berthier, E., Sherpa, S.F., 2016. Reduced melt on debris-covered glaciers: investigations from Changri Nup Glacier, Nepal. Cryosphere 10, 1845–1858. http://dx.doi.org/10.5194/tc-10-1845-2016.

Viviano, G., Salerno, F., Manfredi, E.C., Polesello, S., Valsecchi, S., Tartari, G., 2014. Surrogate measures for providing high frequency estimates of total phosphorus concentrations in urban watersheds. Water Res. 64, 265–277. http://dx.doi.org/10.1016/j.watres.2014.07.009.

Watson, C.S., Quincey, D.J., Carrivick, J.L., Smith, M.W., 2016. The dynamics of supraglacial ponds in the Everest region, central Himalaya. Glob. Planet. Change 142, 14–27. http://dx.doi.org/10.1016/j.gloplacha.2016.04.008.

Yao, T., Thompson, L., Yang, W., Yu, W., Gao, Y., Guo, X., Yang, X., Duan, K., Zhao, H., Xu, B., Pu, J., Lu, A., Xiang, Y., Kattel, D.B., Joswiak, D., 2012. Different glacier status with atmospheric circulations in Tibetan Plateau and surroundings. Nat. Clim. Change 2, 663–667. http://dx.doi.org/10.1038/nclimate1580.

Zhang, Y., Fujita, K., Liu, S.Y., Liu, Q., Nuimura, T., 2011. Distribution of debris thickness and its effect on ice melt at Hailuogou glacier, southeastern Tibetan Plateau, using in situ surveys and ASTER imagery. J. Glaciol. 57, 1147–1157. http://dx.doi.org/10.3189/002214311798843331.

SUPLEMENTARY MATERIAL

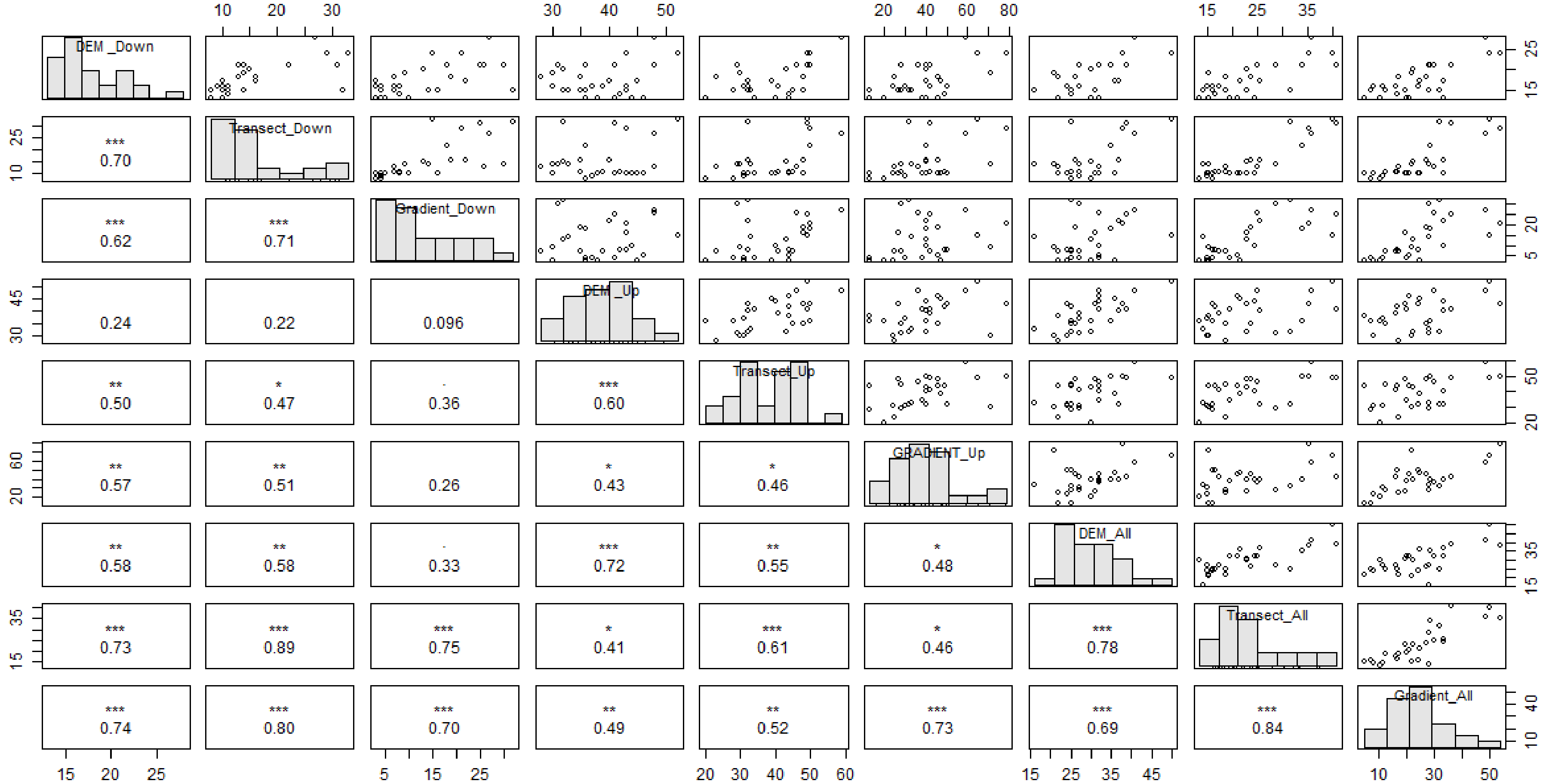

*Figure S1: Correlation matrix referred to different methods to calculate the glacier slope and surface gradient. DEM: mean slope calculated from the DEM; Transect: mean slope calculated along a longitudinal profile (200 m band, as distance); Gradient: surface gradient derived by calculating the angle of a line running from the lowest and the highest part of the glacier (according to Quincey et al, 2007). Down/Up/All refer to the downstream, upstream, and all glacier surface. The coefficient of correlation (r) is plotted with a relevant level of significance (p<0.001 '***'; p<0.01 '**'; p<0.05 '*'; p<0.1 '.').*

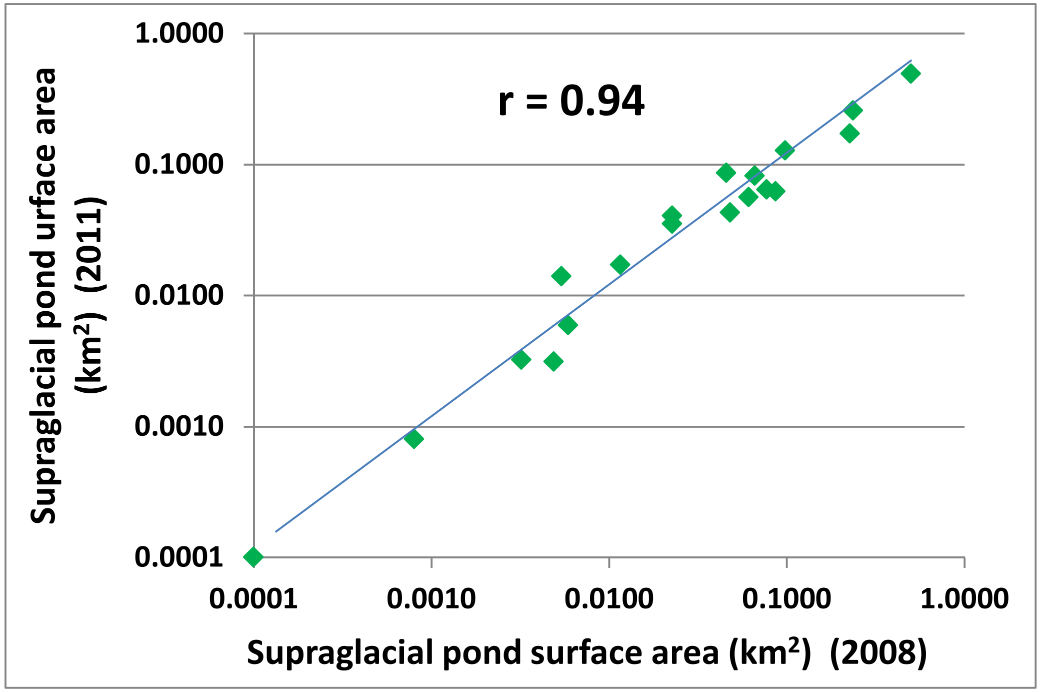

Figure S2: Supraglacial pond surface area of the two analysed post monsoon seasons (24 October 2008 and 30 November 2011)

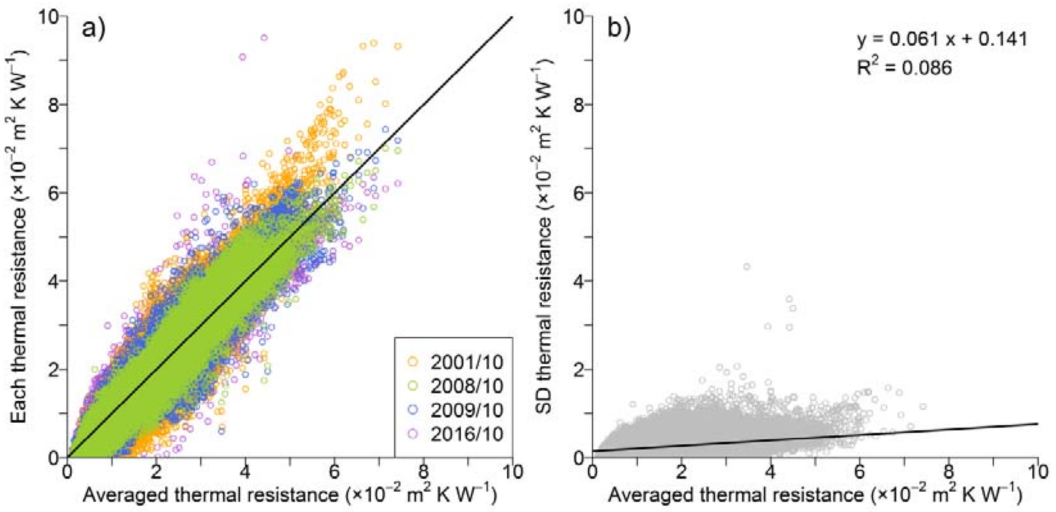

Figure S3: Scatter plots of (a) thermal resistance and (b) standard deviations of multi-temporal Landast data against averaged one.

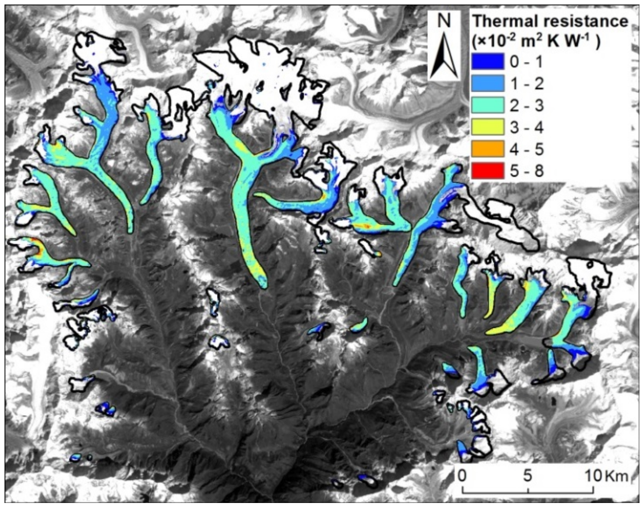

Figure S4: Selected glaciers and spatial distribution of thermal resistance in study area.

*Figure S5: Correlation matrix referred to Figure 2. ΔSURF: Surface area change; ΔSLA: Snow Line Altitude elevation shift; ΔTERM: terminus change; D_Slope: Downstream slope; U_Slope: Upstream slope; DEBR COV: debris coverage; DEBR THCK: debris thickness; Aspect: Glacier aspect expressed as mean deviation from S (see the text); SLA: Snow Line Altitude in 1992; SURF: Glacier surface area in 1992. POND_DENS: Supraglacial pond density. The coefficient of correlation (r) is plotted with a relevant level of significance (p<0.001 '***'; p<0.01 '**'; p<0.05 '*'; p<0.1 '.').*

Table S1: Landsat scene considered for the thermal resistance calculation.

Scene ID	Date	Sensor
LE71400412001290SGS00	17-Oct-01	ETM+
LT51400412008286BJC01	12-Oct-08	TM
LT51400412009288KHC00	15-Oct-09	TM
LC81400412016292LGN00	18-Oct-16	OLI

Table S2: Statistical summary related to the thermal resistance estimation for each glacier.

Name	Min *R* ($\times 10^{-2}$ m^2 K W^{-1})	Max *R* ($\times 10^{-2}$ m^2 K W^{-1})	**Mean *R* ($\times 10^{-2}$ m^2 K W^{-1})**	SD *R* ($\times 10^{-2}$ m^2 K W^{-1})
Amadablam	0.002	4.459	**1.770**	0.746
Bhotekhosi	0.001	6.141	**2.088**	0.732
Chhule	0.010	6.880	**2.555**	1.040
Chhutingpo	0.002	5.126	**1.537**	0.766
Cholo	0.015	6.538	**2.558**	0.893
Cholotse	0.012	3.142	**1.215**	0.696
Duwo	0.003	3.146	**1.693**	0.729
Imja	0.002	5.814	**1.884**	0.919
Kdu_gr125	0.065	4.808	**1.954**	0.810
Kdu_gr181	0.031	0.341	**0.126**	0.079
Kdu_gr38	0.001	4.494	**0.915**	0.962
Khangri	0.002	5.230	**2.322**	0.700
Khumbu	0.005	4.520	**1.768**	0.768
Kyajo	0.067	6.337	**1.621**	1.204
Landak	0.004	4.588	**1.604**	1.032
Langmuche	0.040	3.015	**1.070**	0.822
Lhotse	0.005	4.575	**2.655**	0.679
Lobuche	0.411	4.949	**3.023**	1.090
Lumsamba	0.004	4.969	**2.204**	0.672
Machermo	0.185	4.252	**1.714**	0.703
Melung	0.004	4.583	**2.525**	0.647
Nare	0.000	2.098	**0.964**	0.527
Ngojumba	0.000	11.905	**2.158**	0.829
Nuptse	0.122	4.889	**2.146**	0.567
Phunki	0.002	0.516	**0.204**	0.141
Thyangbo	0.014	3.249	**1.478**	0.920
Tingbo	0.012	1.376	**0.589**	0.418
Wlhotse	0.005	5.977	**2.803**	0.871